

### 23.5 An Inverse-Class-F CMOS VCO with Intrinsic-High-Q 1<sup>st</sup>- and 2<sup>nd</sup>-Harmonic Resonances for 1/f<sup>2</sup>-to-1/f<sup>3</sup> Phase-Noise Suppression Achieving 196.2dBc/Hz FOM

Chee-Cheow Lim<sup>1,2</sup>, Jun Yin<sup>1</sup>, Pui-In Mak<sup>1</sup>, Harikrishnan Ramiah<sup>2</sup>, Rui P. Martins<sup>1,3</sup>

<sup>1</sup>University of Macau, Macau, China

<sup>2</sup>University of Malaya, Kuala Lumpur, Malaysia

<sup>3</sup>Instituto Superior Tecnico/University of Lisboa, Lisbon, Portugal

Second-harmonic common-mode (CM) resonance has been explored for LC oscillators to improve their phase noise (PN) in the past. Its implementation evolves from an explicit design [1] that relies on an extra tail tank, to a recent implicit design [2], where the resonator itself offers a CM impedance peak at 2× the oscillation frequency ( $F_{LO}$ ):

Explicit design (Fig. 23.5.1-upper): a high-Q tail tank ( $Q_{TAIL}$ ) is desirable to raise its impedance  $|Z_{TAIL}|$  at  $2F_{LO}$  and to prevent the loss of  $L_{TAIL}$  from penalizing the PN in the  $1/f^2$  region [3]. To compare with the theoretical limit (FOM<sub>MAX</sub>), the FOM in the  $1/f^2$  PN region is plotted against  $L_{TAIL}$  at different  $Q_{TAIL}$ . Closing the gap between FOM<sub>MAX</sub> and FOM imposes an excessive  $Q_{TAIL}$  of 20 or beyond, which can hardly be achieved and maintained over a wide tuning range.

Implicit design (Fig. 23.5.1-lower): a CM resonance at  $2F_{LO}$  can avoid the physical area and loss of the tail tank. Besides, if the 2<sup>nd</sup>-harmonic current is trapped in the resistive impedance at  $2F_{LO}$  due to the CM resonance, the flicker-noise upconversion can be suppressed [4]. Yet, its practical effectiveness is limited by the presence of PN, which renders both  $F_{LO}$  and  $2F_{LO}$  to drift randomly around their resonances. If the 2<sup>nd</sup>-harmonic current spends more time “trapped” in the resistive part of the tank, the effect of flicker-noise upconversion can be further reduced, but it demands a high-Q impedance at  $2F_{LO}$ . Unfortunately, the implicit CM impedance  $|Z_{CM}|$  is relatively low for two reasons: 1) CM inductance  $L_{CM}=L(1-k)$  is small due to magnetic-flux cancellation and 2) the CM resonance has a low Q at  $2F_{LO}$  up to ~1/4 of its differential-mode counterpart [4] (i.e.  $Q_2/Q_1 \approx 0.25$ ). Although lowering k returns a higher  $Z_{CM}$ , more die area is sacrificed, and the required CM capacitance becomes exceedingly small.

This paper proposes an inverse-Class-F CMOS VCO free of CM resonance. A transformer-based dual-band LC resonator generates two intrinsic-high-Q resonances at  $F_{LO}$  (denoted  $Q_1$ ) and  $2F_{LO}$  (denoted  $Q_2$ ). A high  $Q_2$  corresponds to low PN in both  $1/f^2$  to  $1/f^3$  regions, while the transformer voltage gain aids suppressing the thermal noise contributed by the -g<sub>m</sub> transistors. The high-Q resonances lead to high FOMs at both 100kHz offset (191-to-192.5dBc/Hz) and 10MHz offset (195.6-to-196.2dBc/Hz) over 3.49 to 4.51GHz, while showing low frequency pushing (4.5 to 15MHz/V).

Let us consider a single-ended NMOS VCO using a 1:n transformer (Fig. 23.5.2) to satisfy Barkhausen's criterion. The transformer model [5] reveals that two impedance peaks can be produced despite the VCO being single-ended. To map them at  $F_{LO}$  and  $2F_{LO}$ , we have to satisfy  $16\xi^2 - 68\xi + 100\xi k_m + 16 = 0$  for a mutual coupling factor  $0.3 \leq k_m \leq 0.6$ , where  $\xi$  is the product of the transformer inductance ratio ( $L_S/L_P$ ) and capacitance ratio ( $C_S/C_P$ ), arriving at the inverse-Class-F operation. It implies that the effective inductance at  $F_{LO}$  ( $2F_{LO}$ ) is determined not only by  $L_p$  ( $L_s$ ), but also  $\xi$  and  $k_m$ . Increasing the tank impedance at  $2F_{LO}$  is feasible by sizing  $\xi > 1$ . Based on Fig. 23.5.2, a small  $k_m$  (0.34) is desired to raise  $\xi$  (3.2), leading to a higher  $Q_2/Q_1$  ratio (0.8) than that of [2] by 3.2× and a large transformer voltage gain ( $A_V$ ) resulting in a low-PN VCO design. For a low-power VCO design, a moderate  $\xi$  is desired for a high impedance at  $F_{LO}$ , without disproportionately degrading  $A_V$  and  $Q_2$ .

By stacking such a single-ended NMOS ( $M_N$ ) VCO with its PMOS ( $M_P$ ) counterpart, and merging their respective tanks as a single transformer, an inverse-Class-F CMOS VCO is developed with  $V_{GP}$  and  $V_{GN}$  as the differential outputs (Fig. 23.5.3). Shorting the center taps of the two coils ( $L_s$  and  $L_p$ ) realizes self-biasing at  $V_{DD}/2$ , provided that  $M_p$  and  $M_N$  have a matched large-signal transconductance ( $G_m$ ). The VCO can also be viewed as a 2-port resonator. By ensuring  $M_{P,N}$  are under positive feedback, oscillation only occurs at  $F_{LO}$  even if there is a higher impedance at  $2F_{LO}$  than  $F_{LO}$ .  $C_S$  (5 bits, LSB: 20fF) mainly responds for  $F_{LO}$ , such that  $C_P$  (6 bits, LSB: 11fF) can be tuned for  $F_{LO}$  and  $2F_{LO}$  alignment.

Unlike the differential VCO where the -g<sub>m</sub> transistors are switched on-and-off alternately, here they are switched on (first ½ period) and off (another ½ period) simultaneously. Since the fundamental and 2<sup>nd</sup> harmonic currents are in-phase here (Fig. 23.5.3), when they see their respective resistive paths at  $F_{LO}$  and  $2F_{LO}$  resonances, they result in an asymmetric voltage waveform at the drain, showing a flat span at  $V_{DD}/2$ . A large voltage gain at the gate provided by the transformer drives both  $M_p$  and  $M_N$  into the deep triode region, clipping their drain voltage close to  $V_{DD}$  and 0V, respectively. Using the linear time-variant model [6], the Impulse Sensitivity Function (ISF,  $\Gamma$ ) is around zero at these aforesaid two regions. Hence, the noise factor induced by the tank ( $2\Gamma_{RMS}^2$ ) is lowered from 1 (Class-B & C) to 0.37 (inverse-Class-F). Specifically, the falling and rising times at the drain voltage exhibit different maximum derivatives, resulting in asymmetric ISF between the upper and lower regions. Besides, since channel-length modulation dominates in deep sub-micron CMOS, a harmonically shaped drain voltage gives rise to asymmetric  $G_m$ . Interestingly, the product of a higher  $G_m$  and a lower ISF (and vice versa) in the vicinity of 0 ( $\pi$ ) phase yields a zero DC value for the effective ISF of  $G_m$  and thereby prevents the flicker-noise upconversion.

Due to the presence of harmonic voltages, the FOM of a VCO can be expressed as

$$FOM = 10 \log_{10} \left( \frac{2Q_1^2 \alpha_i \alpha_v}{10^3 kT \Sigma F} \right)$$

where T is the absolute temperature, k is Boltzmann constant,  $\alpha_i = I_{LO}/I_{DC}$  is the current efficiency,  $\alpha_v$  is the voltage efficiency defined as a ratio of the oscillation amplitude at the drain ( $V_{DP,DN}$ ) to  $V_{DD}$ , and  $\Sigma F$  is the total noise factor of the VCO contributed by the resonator and transistors (Fig. 23.5.3). If  $F_{LO}$  and  $2F_{LO}$  can be perfectly aligned at an optimum point of  $C_P=0.57\text{pF}$  and assuming  $\alpha_i=12$ , the calculated FOM (196.3dBc/Hz) of this work is beyond that of Class-F<sub>3</sub> (192.7dBc/Hz at  $\alpha_i=0.63$ ,  $\alpha_v=0.8$  and  $\Sigma F=1.88$ ) and Class-C (192.5dBc/Hz at  $\alpha_i=0.9$ ,  $\alpha_v=0.7$  and  $\Sigma F=2.46$ ). At this point,  $\alpha_i=1.35$  and  $\alpha_v=0.47$ , and  $\Sigma F$  is as low as 1.04 by taking the ISF into account. When  $C_P$  increases slightly, the FOM at  $1/f^2$  region goes up to 196.8dBc/Hz because  $Q_1$  raises before  $\Sigma F$  dominates the degradation. Since  $A_V$  and  $Q_1$  are both function of  $\xi$  [5], FOM<sub>MAX</sub> varies with  $C_P$ . A high  $Q_2$  also benefits the frequency pushing from  $V_{DD}$  caused by the Groszkowski effect. Thus, the frequency pushing of our VCO is only dominated by the inevitable nonlinear capacitances (varactor and parasitic).

The VCO occupies 0.14mm<sup>2</sup> in 65nm CMOS. It utilizes a 2-to-4-turn transformer with  $L_p=2.2\text{nH}$  and  $L_s=4.2\text{nH}$ . The simulated  $Q_1$  is 11.5 and  $Q_2$  is 9.2. Figure 23.5.4 shows the measured PN at 3.49GHz ( $f_{MIN}$ ) and 4.51GHz ( $f_{MAX}$ ). Consistent FOMs at 100kHz offset (191 to 192.5dBc/Hz) and 10MHz offset (195.6 to 196.2dBc/Hz) are achieved. The  $1/f^2$  corner is 100kHz at  $f_{MIN}$  and up to 300kHz at  $f_{MAX}$  due to the AM-PM conversion when the varactor and parasitic capacitance dominate. Figure 23.5.5 shows the PN and FOM plots across the frequency tuning range and its pushing by  $V_{DD}$ . The FOM at  $1/f^2$  region varies within ±0.5dB and peaks to 196.2dBc/Hz. The frequency pushing is 4.5MHz/V at  $f_{MIN}$  dominated by the varactor capacitance and -15MHz/V at  $f_{MAX}$  dominated by the capacitor-bank parasitics. The latter is still 2× lower than that of [2] that is up to 30MHz/V.

Benchmarking with the prior art (Fig. 23.5.6), our inverse-Class-F CMOS VCO exhibits the highest FOMs at both 100kHz and 10MHz offsets over a comparable tuning range, while achieving low frequency pushing, which is among the best reported in Fig. 23.5.6. The die micrograph of the VCO is depicted in Fig. 23.5.7.

#### Acknowledgements:

The authors thank Macau Science and Technology Development Fund (FDCT) - SKL Fund and University of Macau - MYRG2017-00185-AMSV for financial support.

#### References:

- [1] E. Hegazi, et al., “A Filtering Technique to Lower LC Oscillator Phase Noise,” *IEEE JSSC*, vol. 36, no. 12, pp. 1921-1930, Dec. 2001.
- [2] D. Murphy, et al., “Implicit Common-Mode Resonance in LC Oscillators,” *IEEE JSSC*, vol. 52, no. 3, pp. 812-821, Mar. 2017.
- [3] M. Garlampazzi, et al., “Analysis and Design of a 195.6 dBc/Hz Peak FoM P-N Class-B oscillator with Transformer-Based Tail Filtering.” *IEEE JSSC*, vol. 50, no. 7, pp. 1657-1668, July 2015.
- [4] M. Shahmohammadi, et al., “A 1/f Noise Upconversion Reduction Technique Applied to Class-D and Class-F Oscillators,” *ISSCC*, pp. 444-445, Feb. 2015.
- [5] A. Mazzanti and A. Bevilacqua, “On the Phase Noise Performance of Transformer-Based CMOS Differential-Pair Harmonic Oscillators,” *IEEE TCAS-I*, vol. 62, no. 9, pp. 2334-2341, Sept. 2015.
- [6] A. Hajimiri and T. Lee, “A General Theory of Phase Noise in Electrical Oscillators,” *IEEE JSSC*, vol. 33, no. 2, pp. 179-194, Feb. 1998.

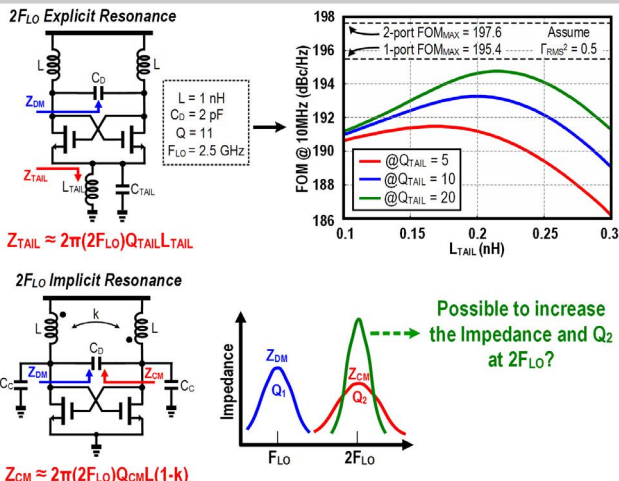


Figure 23.5.1: Upper: VCO with explicit  $2F_{LO}$  resonance [1] and its FOM dependence on  $Q_{TAIL}$ . Lower: VCO with implicit  $2F_{LO}$  resonance [2] to avoid an extra LC tank, but the implicit CM resonance has low impedance and low  $Q$  at  $2F_{LO}$ .

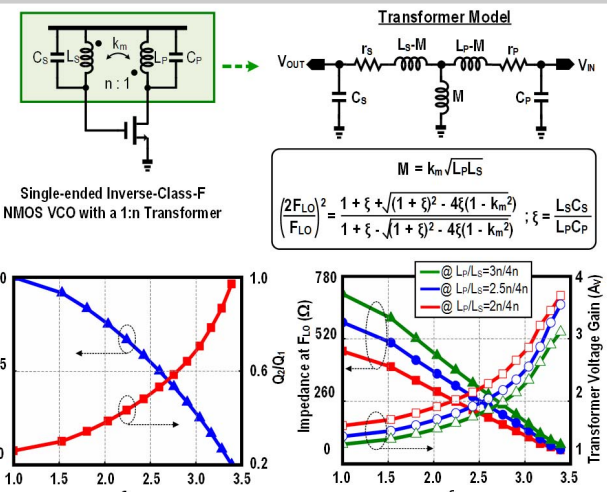


Figure 23.5.2: A single-ended NMOS VCO using a 1: $n$  transformer; the transformer model reveals that 2 impedance peaks can be generated at  $F_{LO}$  and  $2F_{LO}$ .  $\xi=3.2$  and  $k_m=0.34$  yield high  $Q_2/Q_1$  ratio (0.8) and  $A_V$ .

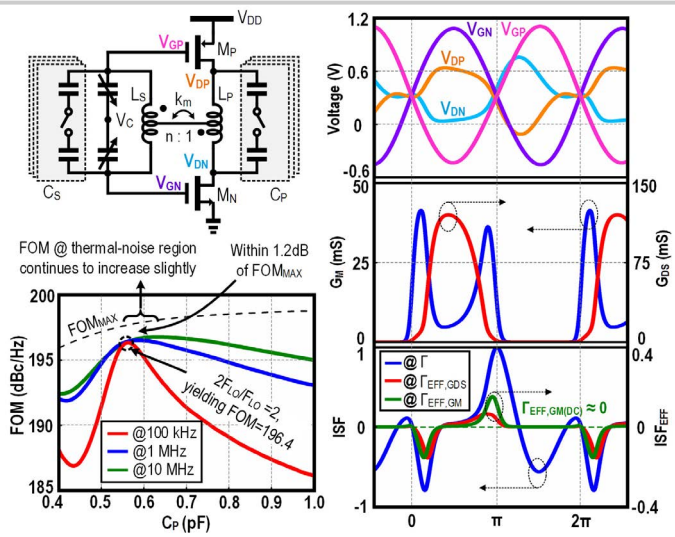


Figure 23.5.3: Proposed inverse-Class-F CMOS VCO. By varying  $C_p$  and  $C_s$ ,  $F_{LO}$  and  $2F_{LO}$  can be aligned to suppress the flicker-noise upconversion.

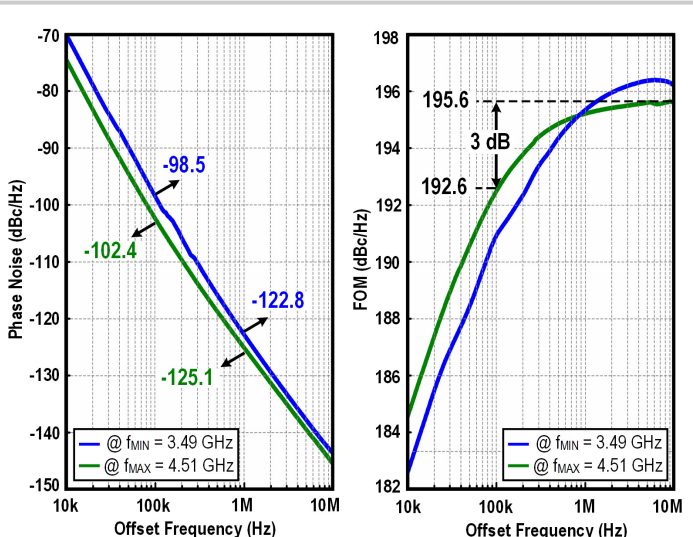


Figure 23.5.4: Measured phase noise and FOM at different offset frequencies.

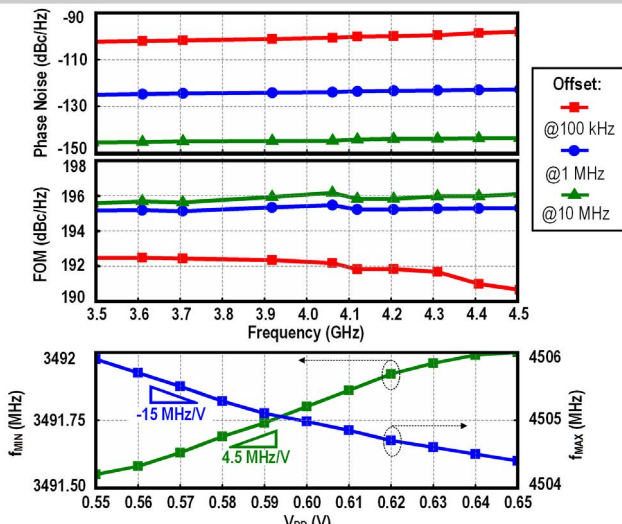


Figure 23.5.5: Upper: Measured phase noise and FOM vs. the oscillation frequency. Lower: Measured frequency pushing at  $f_{MIN}$  and  $f_{MAX}$ .

	This Work	ISSCC'17 [C-C. Li et al.]	JSSC'17 [2]	ISSCC'15 [4]	JSSC'13 [M. Babaei et al.]	JSSC'08 [A. Mazzanti et al.]	JSSC'01 [1]
Topology	CMOS Inverse-Class-F	Trifilar Coil	NMOS CM resonance	Class-F <sub>2,3</sub>	Class-F	Class-C	NMOS+2 $F_{LO}$ tail inductor
CMOS Tech.	65nm	16nm	28nm	40nm	65nm	130nm	0.35μm
Tuning Range	3.49-4.51 (25.5%)	3.2-4.0 (22%)	2.85-3.75 (27.2)	5.4-7 (25%)	2.95-3.8 & (25%)	4.9-5.65 (14%)	1-1.2 (18%)
$V_{DD}$ (V)	0.6	0.4	0.9	1	1.25	1	2.5
Freq. (GHz)	3.49, 4.51	3.23	2.89	5.4	3.7	4.9	1.2
Power (mW)	1.2	1.14	3.8	6.8	12	15	9.1
PN (dBc/Hz) @ 100kHz/10MHz	-102.4/-145.6	-98.5/-143.7	-99 */-145	-108.1/-152	-105.3/-146.7	-103.6/-152.8	-99 */-142 #
FOM (dBc/Hz) @ 100kHz/10MHz	192.5/195.6	191/196.2	183.3/190	188/192.5	189.1/190.5	183.2/192.4	191.3/194.4
Freq. Pushing (MHz/V)	4.5	15	3.6-27.3	6-30	12-23	18-50	N/A
1/f <sup>3</sup> Corner (kHz)	100	300	120	200	60	700	200
Die Area (mm <sup>2</sup> )	0.14	0.11	0.19	0.13	0.12	N/A	N/A

\*Estimated from PN plot   #Normalized from 1 MHz offset   & After on-chip div-by-2

FOM =  $-\text{PN} + 20 \log_{10}(f_0/\Delta f) - 10 \log_{10}(P_{DC}/\text{mW})$

Figure 23.5.6: Performance benchmark with the previously published VCOs.

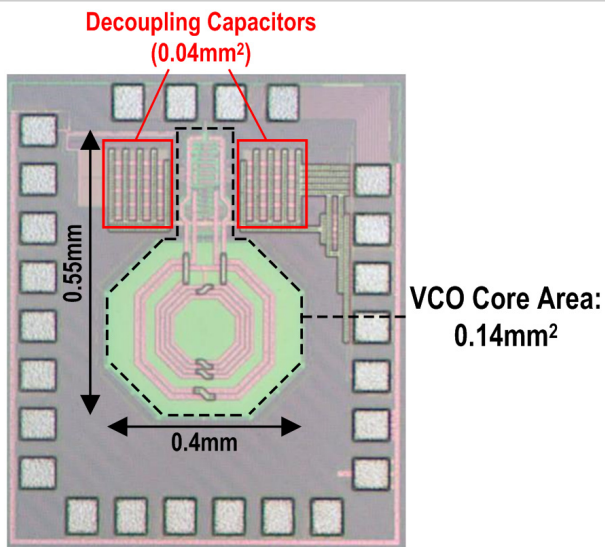


Figure 23.5.7: Die micrograph of the fabricated VCO in 65nm CMOS.